

Differential isospin-fractionation in dilute asymmetric nuclear matter

Bao-An Li,¹ Lie-Wen Chen,^{1,2,3} Hong-Ru Ma,² Jun Xu,² and Gao-Chan Yong^{1,4}

¹*Department of Physics, Texas A&M University-Commerce, Commerce, TX 75429-3011, USA*

²*Institute of Theoretical Physics, Shanghai Jiao Tong University, Shanghai 200240, China*

³*Center of Theoretical Nuclear Physics, National Laboratory of Heavy-Ion Accelerator, Lanzhou, 730000, China*

⁴*Institute of Modern Physics, Chinese Academy of Sciences, Lanzhou 730000, China*

The differential isospin-fractionation (IsoF) during the liquid-gas phase transition in dilute asymmetric nuclear matter is studied as a function of nucleon momentum. Within a self-consistent thermal model it is shown that the neutron/proton ratio of the gas phase becomes *smaller* than that of the liquid phase for energetic nucleons, although the gas phase is overall more neutron-rich. Clear indications of the differential IsoF consistent with the thermal model predictions are demonstrated within a transport model for heavy-ion reactions. Future comparisons with experimental data will allow us to extract critical information about the momentum dependence of the isovector strong interaction.

PACS numbers: 21.65.+f, 21.30.Fe, 24.10.Pa, 64.10.+h

Properties of isospin asymmetric nuclear matter play an important role in understanding many key issues in both nuclear physics and astrophysics [1, 2, 3, 4]. To explore these properties has been one of the major objectives of nuclear sciences. Recent progress and new plans in conducting experiments with more advanced radioactive beams provided us a great opportunity to achieve this goal. Meanwhile, impressive advances have also been made recently in several theoretical fronts in exploring the nature of neutron-rich nucleonic matter and their experimental manifestations. One of the especially interesting new features of a dilute asymmetric nuclear matter is the isospin-fractionation (IsoF) during the liquid-gas (LG) phase transition in it [7, 9, 10, 25]. The non-equal partition of the system's isospin asymmetry with the gas phase being more neutron-rich than the liquid phase has been found as a general phenomenon using essentially all thermodynamical models and in simulations of heavy-ion reactions, for reviews see, e.g., Refs. [1, 5, 6, 11, 12, 13].

In fact, indications of the IsoF have been reported ever since the early 80's although their interpretations have not always been unique [11, 14]. Several recent experiments confirmed unambiguously the IsoF phenomenon [6]. In particular, the experiments and analyses by Xu et al. [15] at the NSCL/MSU are among the most interesting and detailed ones available so far. In their experiments the isotope, isotone and isobar ratios were utilized to obtain an estimate of the neutron/proton density ratio ρ_n/ρ_p in the gas phase at the breakup stage of the reaction. It was found clearly that the gas phase was significantly enriched in neutrons relative to the liquid phase represented by bound nuclei. However, in all of the existing theoretical and experimental studies in the literature, only the average neutron/proton ratios integrated over the nucleon momentum in the liquid and gas phases were studied. We normally refer the above predicted and observed isospin-fractionation as the integrated IsoF. In this work, we investigate the differential IsoF as a function of nucleon momentum. Surprisingly, completely new and very interesting physics is revealed

from the fine structure of the differential IsoF analysis.

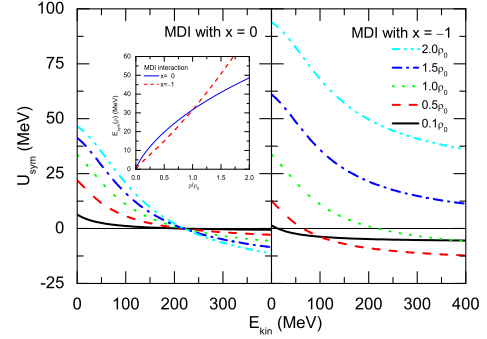


FIG. 1: (Color online) The symmetry potential and energy (insert) in the MDI interaction with $x = 0$ and $x = -1$.

Our study is carried out first within a self-consistent thermal model [16] using the isospin and momentum-dependent MDI interaction [17, 18]. With this interaction, the potential energy density $V(\rho, T, \delta)$ at total density ρ , temperature T and isospin asymmetry $\delta \equiv (\rho_n - \rho_p)/\rho$ is

$$V(\rho, T, \delta) = \frac{A_u \rho_n \rho_p}{\rho_0} + \frac{A_l}{2\rho_0} (\rho_n^2 + \rho_p^2) + \frac{B}{\sigma + 1} \frac{\rho^{\sigma+1}}{\rho_0^\sigma} (1 - x\delta^2) + \sum_{\tau, \tau'} \frac{C_{\tau, \tau'}}{\rho_0} \int \int d^3 p d^3 p' \frac{f_\tau(\vec{r}, \vec{p}) f_{\tau'}(\vec{r}, \vec{p}')}{1 + (\vec{p} - \vec{p}')^2 / \Lambda^2}.$$

In the mean field approximation, Eq. (1) leads to the following single particle potential for a nucleon with momentum \vec{p} and isospin τ

$$U_\tau(\rho, T, \delta, \vec{p}, x) = A_u(x) \frac{\rho^{-\tau}}{\rho_0} + A_l(x) \frac{\rho^\tau}{\rho_0} + B \left(\frac{\rho}{\rho_0} \right)^\sigma (1 - x\delta^2) - 8\tau x \frac{B}{\sigma + 1} \frac{\rho^{\sigma-1}}{\rho_0^\sigma} \delta \rho_{-\tau} + \sum_{t=\tau, -\tau} \frac{2C_{\tau, t}}{\rho_0} \int d^3 \vec{p}' \frac{f_t(\vec{r}, \vec{p}')}{1 + (\vec{p} - \vec{p}')^2 / \Lambda^2}. \quad (2)$$

where $\tau = 1/2$ ($-1/2$) for neutrons (protons), x , $A_u(x)$, $A_\ell(x)$, B , $C_{\tau,\tau}$, $C_{\tau,-\tau}$, σ , and Λ are all parameters given in Ref. [17]. This interaction gives an incompressibility of $K_0 = 211$ MeV for symmetric nuclear matter at saturation density $\rho_0 = 0.16$ fm $^{-3}$. The different x values in the MDI interaction are introduced to vary the density dependence of the nuclear symmetry energy while keeping other properties of the nuclear equation of state fixed [17, 18]. It is worth mentioning that the nucleon isoscalar potential estimated from $U_{\text{isoscalar}} \approx (U_n + U_p)/2$ agrees with the prediction of variational many-body calculations for symmetric nuclear matter [19] in a broad density and momentum range [17]. The corresponding isovector (symmetry) potential can be estimated from $U_{\text{sym}} \approx (U_n - U_p)/2\delta$. With both $x = 0$ and $x = -1$ at normal nuclear matter density, the symmetry potential agrees very well with the Lane potential extracted from nucleon-nucleus and (n,p) charge exchange reactions available for nucleon kinetic energies up to about 100 MeV [17, 20]. At abnormal densities and higher nucleon energies, however, there is no experimental constrain available at present.

The isospin diffusion data from the NSCL/MSU [21] have recently constrained the value of x to be between 0 and -1 at sub-saturation densities [18, 22]. Shown in the insert of Fig. 1 is the density dependent symmetry energy $E_{\text{sym}}(\rho)$ with $x = 0$ and $x = -1$, respectively. While this constraint on the $E_{\text{sym}}(\rho)$ is the most stringent achieved so far in the field, the corresponding symmetry potential shown in Fig. 1 still diverges much more widely with both momentum and density. This is not surprising. Comparing Eqs. (1) and (2), it is seen that the symmetry energy obtained using Eq. (1) involves the integration of the single nucleon potential over its momentum. To obtain information about the underlying momentum- and density-dependence of the symmetry potential which is more fundamental than the $E_{\text{sym}}(\rho)$ for many important physics questions, one thus has to use differential probes. We will demonstrate that the differential IsoF as a function of nucleon momentum is such an observable.

The phase space distribution function f_τ is the Fermi distribution

$$f_\tau(\vec{r}, \vec{p}) = \frac{2}{h^3} \left[\exp\left(\frac{p^2}{2m_\tau} + U_\tau - \mu_\tau}{T}\right) + 1 \right]^{-1} \quad (3)$$

where μ_τ is the proton or neutron chemical potential determined self-consistently from $\rho_\tau = \int f_\tau(\vec{r}, \vec{p}) d^3p$. In the above, m_τ is the proton or neutron mass. From a self-consistency iteration scheme [16, 23], the chemical potential μ_τ and the distribution function $f_\tau(\vec{r}, \vec{p})$ are determined numerically.

From the chemical potential μ_τ and the distribution function $f_\tau(\vec{r}, \vec{p})$, the energy per nucleon $E(\rho, T, \delta)$ can be obtained as

$$E(\rho, T, \delta) = \frac{1}{\rho} \left[V(\rho, T, \delta) + \sum_\tau \int d^3p \frac{p^2}{2m_\tau} f_\tau(\vec{r}, \vec{p}) \right]. \quad (4)$$

Furthermore, the entropy per nucleon $S_\tau(\rho, T, \delta)$ is obtained from

$$S_\tau(\rho, T, \delta) = -\frac{8\pi}{\rho h^3} \int_0^\infty p^2 [n_\tau \ln n_\tau + (1-n_\tau) \ln(1-n_\tau)] dp \quad (5)$$

with the occupation probability $n_\tau = \frac{h^3}{2} f_\tau(\vec{r}, \vec{p})$. Finally, the pressure $P(\rho, T, \delta)$ is calculated from the thermodynamic relation

$$P(\rho, T, \delta) = \left[T \sum_\tau S_\tau(\rho, T, \delta) - E(\rho, T, \delta) \right] \rho + \sum_\tau \mu_\tau \rho_\tau. \quad (6)$$

For the ease of following discussions, we first reproduce the integrated IsoF using the above formalism. In hot asymmetric nuclear matter, the LG phase coexistence is governed by the Gibbs conditions

$$\mu_i^L(T, \rho_i^L) = \mu_i^G(T, \rho_i^G), \quad (i = n \text{ and } p) \quad (7)$$

$$P_i^L(T, \rho_i^L) = P_i^G(T, \rho_i^G), \quad (i = n \text{ or } p). \quad (8)$$

At any given pressure below the critical point, the two solutions for the liquid and gas phases thus form the edges of a rectangle in the proton and neutron chemical potential isobars as a function of isospin asymmetry δ and can be found by means of the standard geometrical construction method [16].

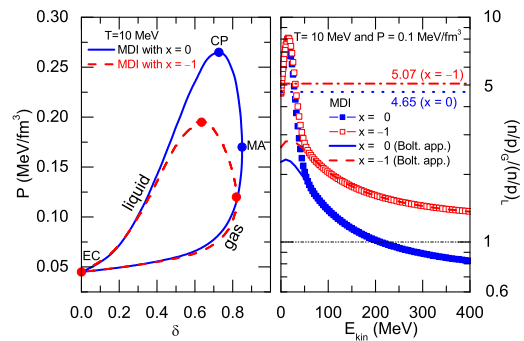


FIG. 2: (Color online) Left window: the section of binodal surface at $T = 10$ MeV with $x = 0$ and $x = -1$. The critical point (CP), the points of equal concentration (EC) and maximal asymmetry (MA) are also indicated. Right window: the double neutron/proton ratio in the gas and liquid phases $(n/p)_G/(n/p)_L$ as a function of the nucleon kinetic energy.

Shown in the left window of Fig. 2 is a typical section of the binodal surface at $T = 10$ MeV with $x = 0$ and $x = -1$. The phenomenon of integrated IsoF with the gas phase being more neutron-rich is seen very clearly. It is also seen that the stiffer symmetry energy ($x = -1$) significantly lowers the critical point (CP). However, below a pressure of about $P = 0.12$ MeV/fm 3 , the magnitude of the integrated IsoF becomes almost independent of the symmetry energy used. To examine the advantages of the differential IsoF analyses over the integrated ones, as an example, we select the gas and liquid phases

in equilibrium at $T=10$ MeV and $P = 0.1$ MeV/fm³. For $x = 0$ the density and isospin asymmetry are, respectively, $\rho_G = 0.087\rho_0$ and $\delta_G = 0.791$ for the gas phase, and $\rho_L = 0.763\rho_0$ and $\delta_L = 0.296$ for the liquid phase. For $x = -1$ they are, respectively, $\rho_G = 0.114\rho_0$, $\delta_G = 0.808$, $\rho_L = 0.714\rho_0$ and $\delta_L = 0.30$. The corresponding double neutron/proton ratio in the gas and liquid phases $\frac{(n/p)_G}{(n/p)_L}(p)$ can then be readily obtained using Eq. (3) as a function of nucleon momentum or kinetic energy. We refer this function as the differential IsoF.

Shown in the right window of Fig. 2 are the differential IsoFs for both $x = 0$ and $x = -1$. It is interesting to see that the isospin-fractionation is strongly momentum dependent. Moreover, while the integrated double neutron/proton ratios of 5.07 ($x = -1$) and 4.65 ($x = 0$) are very close to each other, the differential IsoF for nucleons with kinetic energies high than about 50 MeV is very sensitive to the parameter x used. Surprisingly, a reversal of the normal IsoF is seen for $x = 0$ for nucleons with kinetic energies higher than about 220 MeV. In this case, there are more energetic neutrons than protons in the liquid phase compared to the gas phase. We note that at pressures higher than 0.1 MeV/fm³ where the integrated IsoF is already very sensitive to the $E_{sym}(\rho)$, the differential IsoF is much more sensitive to the x parameter than that shown in Fig. 2. For energetic nucleons where the differential IsoF is very sensitive to the parameter x , the f_τ can be well approximated by the Boltzmann distribution as shown in Fig. 2. For these nucleons in either the liquid (L) or gas (G) phase, the neutron/proton ratio

$$(n/p)_{L/G} = \exp[-(E_n^{L/G} - E_p^{L/G} - \mu_n^{L/G} + \mu_p^{L/G})/T]. \quad (9)$$

The energy difference of neutrons and protons having the same kinetic energy and mass

$$E_n^{L/G} - E_p^{L/G} = U_n^{L/G} - U_p^{L/G} \approx 2\delta_{L/G} \cdot U_{sym}(p, \rho_{L/G}) \quad (10)$$

is directly related to the symmetry potential U_{sym} . Because of the chemical equilibrium conditions given in Eq. (7), the chemical potentials cancel out in the double neutron/proton ratio

$$\frac{(n/p)_G}{(n/p)_L}(p) = \exp[-2(\delta_G \cdot U_{sym}(p, \rho_G) - \delta_L \cdot U_{sym}(p, \rho_L))/T]. \quad (11)$$

This general expression clearly demonstrates that the differential IsoF for energetic nucleons carries direct information about the momentum dependence of the symmetry potential. In the above expressions, the tiny temperature dependence of the symmetry potential has been neglected.

For both the liquid-gas and hadron-QGP (quark-gluon-plasma) phase transitions, equilibrium model calculations for infinite nuclear matter are very useful for developing new concepts and predicting novel phenomena. However, the experimental search/confirmation for the new phenomena/concepts in real nuclear reactions is usually very challenging. For example, the intermediate energy heavy-ion reaction community has been studying for

more than two decades the underlying nature and experimental signatures of the LG phase transition predicted first for infinite nuclear matter based on thermodynamical considerations. Hopefully, similar to the very fruitful study recently in momentum-space about how electrons behave during the phase transition to high-temperature superconductors[24], the new study about how nucleons behave in the correlated momentum- and isospin-space may reveal deeper insights into the nature of the LG phase transition.

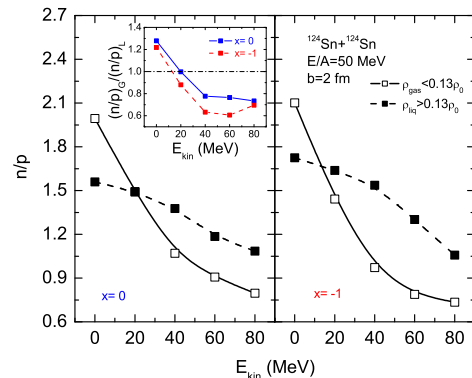


FIG. 3: (Color online) The neutron/proton ratio in the “gas” and “liquid” phases as a function of the nucleon kinetic energy for the reaction of $^{124}\text{Sn}+^{124}\text{Sn}$ at $E_{beam}/A = 50$ MeV.

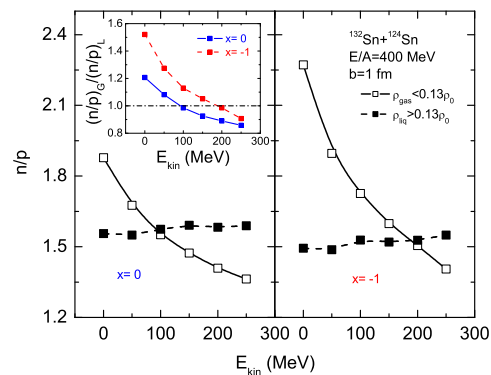


FIG. 4: (Color online) Same as Fig. 3 but for the reaction of $^{132}\text{Sn}+^{124}\text{Sn}$ at $E_{beam}/A = 400$ MeV.

How can one experimentally measure the differential IsoF? As for the structure functions of quarks and gluons in the initial state of relativistic heavy-ion collisions, the momentum distribution of the n/p ratio in the liquid phase may not be measured directly since what can be detected at the end of heavy-ion reactions are free nucleons and bound nuclei in their ground states. Nevertheless, precursors and/or residues of the transition in the differ-

ential IsoF may still be detectable in heavy-ion reactions especially those induced by radioactive beams. While a comprehensive study on the detailed signatures of the differential IsoF is beyond the scope of this work, we have actually performed calculations using the IBUU04 transport model with the same MDI interaction[17]. Shown in Fig. 3 and Fig. 4 are two typical examples for the central reaction of $^{124}\text{Sn}+^{124}\text{Sn}$ at $E_{beam}/A = 50$ MeV and $^{132}\text{Sn}+^{124}\text{Sn}$ at $E_{beam}/A = 400$ MeV, respectively. To separate approximately nucleons in the low density “gas” region from those in the “liquid” region a density cut at $0.13\rho_0$ is used. Calculations using a cut at $0.5\rho_0$ in the reaction at 50 MeV/A lead to qualitatively the same although quantitatively slightly different results. Very interestingly, in both reactions there is indeed a transition from the neutron-richer (poorer) “gas (liquid)” phase normally known as the IsoF for low energy nucleons to the opposite behavior (i.e., anti-IsoF) for more energetic ones. Moreover, the transition nucleon energy from the normal IsoF to the anti-IsoF is sensitive to the parameter x used. This is more pronounced in the reaction at $E_{beam}/A = 400$ MeV where effects of the symmetry (Coulomb) potential are relatively stronger (weaker) for more energetic nucleons consistent with predictions of the thermal model in the right window of Fig. 2. Comparing the thermal model predictions and the transport model results, one sees that the two independent approaches predict qualitatively the same phenomenon while there are quantitative differences, especially for low energy nucleons. This is mainly because in nuclear reactions the Coulomb repulsion shifts protons in the gas phase from low to higher energies leading to the peak in $(n/p)_G$ ratio at $E_{kin} = 0$, while it has little effects on the protons in the liquid phase. Transport model calculations without the Coulomb potential lead to results more closely resembling the thermal model predictions for infinite nuclear matter. We notice that the “gas” phase defined in this

study contains also the pre-equilibrium nucleons which are known to be more neutron-rich than the reaction system[25]. They are energetic and thus affect mostly the high energy part of the $(n/p)_G$ ratio. The subtraction of the pre-equilibrium nucleons from our analyses will thus mainly lower the $(n/p)_G$ for high energy nucleons. Therefore, the transition from the normal IsoF to the anti-IsoF will become more obvious and it will make our conclusions even stronger. We also notice that the radial flow affects all nucleons in both the gas and liquid phases the same way as already illustrated in ref.[26]. The subtraction of the radial flow is expected to have very little effect on the neutron/proton ratio.

In summary, the differential IsoF is studied as a function of nucleon momentum. While the gas phase is overall more neutron-rich than the liquid phase, the gas phase is richer (poorer) only in low (high) energy neutrons than the liquid phase. Clear indications of the differential IsoF consistent with the thermodynamic model predictions are demonstrated within a transport model for heavy-ion reactions. While it may be very challenging to test experimentally the predictions, future comparisons with experimental data will allow us to extract critical information about the momentum dependence of the isovector strong interaction.

We would like to thank Drs. Wei-Zhou Jiang, Yang Sun and Wolfgang Trautmann for helpful discussions. This work was supported in part by the US National Science Foundation under Grant No. PHY-0652548 and the Research Corporation under Award No. 7123, the National Natural Science Foundation of China under Grant Nos. 10334020, 10575071, and 10675082, MOE of China under project NCET-05-0392, Shanghai Rising-Star Program under Grant No. 06QA14024, the SRF for ROCS, SEM of China, and the China Major State Basic Research Development Program under Contract No. 2007CB815004.

-
- [1] B.A. Li, C.M. Ko, and W. Bauer, *Int. Jour. Mod. Phys. E* **7**, 147 (1998).
[2] P. Danielewicz, R. Lacey, and W. G. Lynch, *Science* **298**, 1592 (2002).
[3] J.M. Lattimer and M. Prakash, *Science* **304**, 536 (2004).
[4] A. W. Steiner *et al.*, *Phys. Rep.* **411**, 325 (2005).
[5] *Isospin Physics in Heavy-Ion Collisions at Intermediate Energies*, Eds. Bao-An Li and W. Udo Schröder (Nova Science Publishers, Inc, New York, 2001).
[6] *Dynamics and Thermodynamics with Nucleonic Degrees of Freedom*, Eds. Ph. Chomaz, F. Gulminelli, W. Trautmann and S.J. Yennello, Springer, (2006).
[7] H. Müller and B.D. Serot, *Phys. Rev. C* **52**, 2072 (1995).
[25] B.A. Li and C.M. Ko, *Nucl. Phys.* **A618**, 498 (1997).
[9] V. Baran *et al.*, *Nucl. Phys.* **A632**, 287 (1998).
[10] B.A. Li, *Phys. Rev. Lett.* **85**, 4221 (2000).
[11] Ph. Chomaz *et al.*, *Phys. Rep.* **389**, 263 (2004).
[12] C.B. Das *et al.*, *Phys. Rep.* **406**, 1 (2005).
[13] V. Baran *et al.*, *Phys. Rep.* **410**, 335 (2005).
[14] J. Randrup and S.E. Koonin, *Nucl. Phys.* **A356**, 223 (1981).
[15] H.S. Xu *et al.*, *Phys. Rev. Lett.* **85**, 716 (2000).
[16] J. Xu *et al.*, *Phys. Rev. C* **75**, 014607 (2007); *Phys. Lett.* **B650**, 348 (2007).
[17] C. B. Das *et al.*, *Phys. Rev. C* **67**, 034611 (2003); B.A. Li *et al.*, *Nucl. Phys.* **A735**, 563 (2004).
[18] L.W. Chen, C.M. Ko, and B.A. Li, *Phys. Rev. Lett.* **94**, 032701 (2005).
[19] R.B. Wiringa, *Phys. Rev. C* **38**, 2967 (1988).
[20] P.E. Hodgson, *The Nucleon Optical Model*, pages 613-651, (World Scientific, Singapore, 1994).
[21] M.B. Tsang *et al.*, *Phys. Rev. Lett.* **92**, 062701 (2004).
[22] B.A. Li and L.W. Chen, *Phys. Rev. C* **72**, 064611 (2005).
[23] C. Gale *et al.*, *Phys. Rev. C* **41**, 1545 (1990).
[24] M. Norman, *Science* **303**, 1985 (2004).
[25] B.A. Li *et al.* *Phys. Rev. Lett.* **78**, 1644 (1997).
[26] B.A. Li, G.C. Yong and W. Zuo, *Phys. Rev. C* **71**, 044604 (2005).